Published in final edited form as:

Ocul Surf. 2022 October ; 26: 234–243. doi:10.1016/j.jtos.2022.10.001.

Imbalanced IL-37/TNF-α/CTSS signaling disrupts corneal epithelial barrier in a dry eye model in vitro

Yun Zhang[a,b,1], **Jin-Miao Li**[a,c,1], **Rong Lu**[c], **Zhao Liu**[a], **Xin Chen**[a,b], **Cintia S. de Paiva**[a], **Stephen C. Pflugfelder**[a], **De-Quan Li**[a,*]

[a]Ocular Surface Center, Cullen Eye Institute, Department of Ophthalmology, Baylor College of Medicine, Houston, TX, USA

[b]School of Optometry and Ophthalmology, Eye Hospital, Wenzhou Medical University, Wenzhou, China

[c]State Key Laboratory of Ophthalmology, Zhongshan Ophthalmic Center, Guangzhou, China

Abstract

Purpose: To explore novel role and molecular mechanism of a natural anti-inflammatory cytokine interleukin (IL) 37 in preventing corneal epithelial barrier disruption from hyperosmolar stress as can occur in dry eye disease.

Methods: Primary human corneal epithelial cells (HCECs) were cultured from fresh donor limbal explants. An in vitro dry eye model with hyperosmolar stress was established by switching HCECs from isosmolar (312mOsM) to hyperosmolar medium (350–500 mOsM), and some cells were treated with rhIL-37 or rhTNF-α, for different periods (2–48 h). The expression of cytokines and cathepsin S, and barrier protein integrity were evaluated by RT-qPCR, ELISA, and immunofluorescent staining with confocal microscopy.

Results: The integrity of epithelial barrier was significantly disrupted in HCECs exposed to hyperosmolar medium, as shown by immunofluorescent images of tight junction (TJ, ZO-1, occludin and claudin-1) and adheren junction (E-cadherin) proteins. TNF-α accentuated hyperosmolar-induced disruption of TJ barrier functional integrity whereas exposure to IL-37 blunted or even reversed these changes. Cathepsin S, encoded by CTSS gene, was found to directly disrupt epithelial barrier integrity. Interestingly, CTSS expression was significantly induced by TNF-α and hyperosmolarity, while exogenous rhIL-37 inhibited TNF-α and CTSS expression at mRNA and protein levels following hyperosmolar stress. Furthermore, rhIL-37 restored barrier protein integrity, observed in 2D and 3D confocal immunofluorescent images, in HCECs under hyperosmolar stress.

*Corresponding author. Ocular Surface Center, Cullen Eye Institute, Department of Ophthalmology, Baylor College of Medicine, Houston, TX, 77030, USA. dequanl@bcm.edu (D.-Q. Li).

[1]These authors contributed equally to this work.

Author contributions

D-Q.L., R.L., and S.C.P. designed the research, Y.Z., J-M.L., Z.L., and X.C. conducted the experiments, Y.Z., J-M.L., R.L, C.S.P, and D-Q.L. analyzed the results, Y.Z., J-M.L. and D-Q.L. wrote the manuscript, S.C. P. performed English editing, all authors reviewed the manuscript.

Declaration of competing interest

The authors declare no competing interests.

Conclusion: Our findings demonstrate a novel signaling pathway by which anti-inflammatory cytokine IL-37 prevents corneal epithelial barrier disruption under hyperosmotic stress via suppressing TNF-α and CTSS expression. This study provides new insight into mechanisms protecting corneal barrier in dry eye disease.

Keywords

Corneal barrier; CTSS; Dry eye; Hyperosmolarity; IL-37; Tight junction; Adheren junction; Epithelium

1. Introduction

The integrity of epithelial barrier is crucial for maintaining tissue homeostasis and protecting host tissues from environmental toxins, pollutants, allergens and infections. The increasing research investigations indicates that a defective epithelial barrier in skin and mucosal tissues is an important factor in the pathogenesis of allergic, autoimmune, and other chronic inflammatory diseases, such as asthma, atopic dermatitis, allergic rhinitis, eosinophilic esophagitis, and inflammatory bowel disease [1–8].

In addition, disruptive leaky barrier and microbial dysbiosis in the gut contribute to remote tissue inflammation and systemic autoimmune and metabolic diseases, including diabetes, obesity, rheumatoid arthritis, multiple sclerosis, and systemic lupus erythematosus [9–12]. Furthermore, gut barrier defects and microbial translocation have also been found to associate with neurodegenerative conditions such as Parkinson's and Alzheimer disease, or psychiatric disorder such as depression [13–15].

A review article published in 2021 authored by Dr. Akdis proposes an extended "epithelial barrier hypothesis" that the increase in epithelial barrier-damaging agents linked to industrialization, urbanization and modern life underlies the rise in allergic, autoimmune and other chronic conditions [16].

Epithelial barrier disruption has been also observed in ocular surface inflammatory diseases, including allergic, autoimmune conditions, and dry eye [17–20]. We have observed that IL-33/ST-2/IL-9/IL-9R signaling mediates pollen-induced allergic conjunctivitis in a murine model [21]. Dry eye is the most prevalent chronic ocular surface inflammatory disease. Epithelial barrier hypothesis may well explain why the prevalence of dry eye syndrome is increasing rapidly in industrialized countries and modern life. Corneal epithelial barrier disruption has been recognized as an important pathogenic factor leading to chronic inflammation in dry eye. However, the molecular mechanisms by which the corneal epithelial barrier becomes disrupted warrant further studies to advance our understanding of the leaky barrier in dry eye.

Tear hyperosmolarity and proinflammatory mediators such as cytokines, chemokines and metalloproteinases have been recognized to induce dry eye disease symptoms and cause damage to epithelial barrier function. The role and mechanism of natural anti-inflammatory cytokines in protecting ocular surface from inflammation and barrier disruption are not well known.

The interleukin (IL)-1 family is a group of 11 pro- and anti-inflammatory cytokines. A new member IL-37, also named as IL-1F7, is a natural anti-inflammatory cytokine. IL-37 is expressed in various tissues and cells, including epithelial cells, monocytes, macrophages, dendritic and $CD4^+$ T cells. It functions as a fundamental inhibitor of innate inflammation and immunity. It plays a vital role in regulating inflammatory responses by suppressing the expression, production and function of proinflammatory cytokines [22,23]. The protective roles of IL-37 have been recognized in a variety of inflammatory and autoimmune diseases, such as asthma, psoriasis, rheumatoid arthritis, inflammatory bowel disease, Graves' disease and systemic lupus erythematosus [24–29]. IL-37 has been shown to exert antitumor effects, and it may act as a prognostic marker in some human cancers [30,31].

Nevertheless, the effects of IL-37 on protecting mucosal epithelial barrier from inflammation in ocular disease such as dry eye has not been reported. To further understand the epithelial barrier hypothesis in dry eye, this study explored whether IL-37 cytokine is expressed by corneal epithelium, and how it functions in protecting corneal epithelial barrier from inflammation-mediated disruption in an in vitro culture model of dry eye, which uses primary human corneal epithelial cells (HCECs) exposed to hyperosmolar stress.

2. Methods

2.1. Materials and reagents

The culture supplies such as Dulbecco modified Eagle medium (DMEM), Ham-F12, Cortisone, EGF, gentamicin, and amphotericin B, TaqMan gene expression assays and real-time PCR master mix, the rabbit polyclonal antibodies against human zonula occludens (ZO)-1, occludin, claudin-1 and E-cadherin, as well as IL-37 Human ELISA Kit, were purchased from Thermo Fisher Scientific (Waltham, MA). Fetal bovine serum (FBS) was from Hyclone (Logan, UT). RNeasy Plus Mini RNA extraction kit from Qiagen (Valencia, CA). Ready-To-Go You-Prime First-Strand Beads were from GE Healthcare (Piscataway, NJ). Fluorescein Alexa-Fluor 488-conjugated secondary antibodies (goat anti rabbit IgG) were from Molecular Probes (Eugene, OR). Recombinant human (rh) IL-37 and TNF-α were from ProSpec (East Brunswick NJ). ELISA kit for human TNF-α was from BioLegend (San Diego, CA), and Cathepsin S from Boster Bio (Pleasanton, CA). All plastic ware was purchased from Becton Dickinson Biosciences (Lincoln Park, NJ).

2.2. Primary HCEC culture and in vitro dry eye model with hyperosmolarity

Human corneal tissues not suitable for transplantation were obtained from the Lions Eye Bank of Texas (Houston, TX). Primary HCECs were established from donor limbal tissues using explant cultures in a supplemented hormonal epidermal medium (SHEM) containing 10% FBS as our previous publications [32]. We only used the confluent cultures, which showed the phenotype of corneal epithelial cells without visible fibroblasts, as previously reported [32–35].

Hyperosmolar stress model was established by switching the confluent HCECs from isosmolar (312 mOsM) to hyperosmolar medium at 350, 400, 450 and 500 mOsM, which was achieved by adding 19, 44, 69 or 94 mM of sodium chloride, respectively [36–39].

The culture medium osmolarity was measured by a vapour pressure osmometer in the Body Fluids Clinical Chemistry Laboratory of the Houston Methodist Hospital (Houston, TX). The HCECs exposed to 450 mOsM for 2, 4, 8 and 24 h were used for time course of mRNA expression, and the cultures treated 350, 400, 450 and 500 mOsM for 4 and 24 h were used for osmolarity-dependent response assays. For gene expression assay, the cells were treated for 4 h and then lysed in buffer RLT from the Qiagen RNeasy Plus Mini kit for total RNA extraction. The HCECs treated for 24–48 h were used for immunofluorescent staining and enzyme-linked immunosorbent assay (ELISA). Each experiment was repeated five times.

2.3. Differential regulation of IL-37, TNF-α and cathepsin S in HCECs

To evaluate differential response of HCECs under hyperosmolar stress, the confluent human corneal epithelial cultures in 12-well plates were switched to hyperosmolar medium (350–500 mOsM) for 4–24 h with or without rhIL-37 (1–20 ng/ml), and some cells were treated with rhTNF-α (1–20 ng/ml), with untreated cultures used as isosmolar controls. The control and treated cells were used for mRNA and protein assays. Each experiment was repeated three to five times.

2.4. Human corneal epithelial barrier disruption by hyperosmolarity and cathepsin S treatment

For barrier disruption assays, primary HCECs were cultured in 8-chamber slides from limbal explants in SHEM using our previously reported method [21]. Confluent corneal epithelial cultures were exposed to hyperosmolar medium, or treated with cathepsin S at 100–400 ng/ml, in the absence or presence of cathepsin S inhibitor LY3000328 or rhIL-37 for 48 h. The untreated cultures were used as isosmolar controls. Immunofluorescent staining for barrier proteins was then performed. Each experiment was repeated at least three times.

2.5. RNA extraction, reverse transcription (RT), and quantitative real-time PCR (RT-qPCR)

Total RNA was extracted with RNeasy Plus Mini Kit according to the manufacturer's instructions, quantified with a spectrophotometer (NanoDrop ND-1000; Thermo Scientific, Wilmington, DE), and stored at −80 °C before use. The first strand cDNA was synthesized by RT from 2.0 μg of total RNA using Ready-To-Go You-Prime First-Strand Beads as previously described [40].

Quantitative real-time PCR was performed in the QuantStudio® 3 Real-Time PCR System (Applied Biosystems, Foster City, CA) with a 10 μl reaction volume containing 4.5 μl of cDNA, 0.5 μl TaqMan gene expression assay, and 5 μl TaqMan gene expression master mix. The thermocycler parameters were 50 °C for 2 min and 95 °C for 10 min, followed by 35 cycles of 95 °C for 15 s and 60 °C for 1 min. TaqMan gene expression assays used for this study were: GAPDH (Hs99999905_m1), TNF-α (Hs00174128_m1), IL-37 (Hs00367201_m1), and CTSS (Hs00175407_m1). A non-template control was included to evaluate DNA contamination. The results were analyzed by the comparative threshold cycle (Ct) method and normalized by GAPDH as an internal control [41,42].

2.6. Enzyme-linked immunosorbent assays (ELISA)

Double-sandwich ELISA for human TNF-α, cathepsin S and IL-37 was performed to determine their protein concentrations in the conditioned media and cells from different treatments according to manufacturer's protocols and our previously reported methods [37]. Absorbance was read at 450 nm with a reference wavelength of 570 nm by Infinite M200 microplate reader (Tecan US, Inc., Morrisville, NC).

2.7. Immunofluorescent staining and laser scanning confocal microscopy

Using a previously reported method [21], HCECs on 8-chamber slides were fixed with cold acetone at − 30 °C for 3 min. After blocking with 20% normal goat serum in PBS for 30 min, the samples were incubated with primary antibodies overnight at 4 °C. The primary antibodies were rabbit anti-human ZO-1, occludin, claudin-1, E-cadherin, TNF-α or cathepsin S. Alexa-Fluor 488 (1:200) conjugated secondary antibody and DAPI for nuclear counterstaining were used. The 2D and 3D digital images were captured with a laser scanning confocal microscope (Nikon A1 RMP, Nikon, Melville, NY) wavelength 400–750 nm and one μm z-step. The images were processed using NIS Elements software, version 4.20 (Nikon, Garden City, NY).

2.8. Statistical analysis

Student t-test or Mann-Whitney *U* test was used to make comparisons between 2 groups.

One-way ANOVA test was used to make comparisons among three or more groups, followed by Dunnett's post-hoc test. $P \leq 0.05$ was considered statistically significant.

3. Results

3.1. Corneal epithelial barrier was disrupted by hyperosmolar stress

Mucosal epithelial barrier is formed with apical junctional complexes consisting of the apical tight junctions and underlying adheren junctions [18,43–46]. In this in vitro dry eye model, barrier integrity was evaluated in primary HCECs exposed to hyperosmolar medium at 450 mOsM for different time periods, and exposed to different osmolarities for 48 h, using cells cultured in isosmolar medium (312 mOsM) as controls.

We observed that hyperosmolar medium at 450 mOsM for 24 and 48 h significantly and time-dependently disrupted tight junction proteins ZO-1, occludin and claudin-1, as well as adheren junction protein E-cadherin, as shown morphologically by immunofluorescent staining in Fig. 1A. The disruption of these four barrier proteins was also found to be osmolarity-dependent in HCECs exposed to 400, 450 and 500 mOsM for 48 h (Fig. 1B). It appears that cells significantly lose barrier integrity when subjected to 450 mOsM for 48 h, which is the optimal condition used for the following experiments.

3.2. The opposing effects of hyperosmolar stress on TNF-α and IL-37 expression levels in HCECs

The confluent HCEC cultures were switched to medium with higher osmolarities ranging from 350 to 500 mOsM for 2–24 h and compared to cells cultured in isosmolar medium as

controls. As shown in Fig. 2A, mRNA expression of the proinflammatory cytokine TNF-α mRNA was dramatically induced at 2 h, reached peak levels at 4 h, and was sustained for at least 24 h. Its expression levels were stimulated in an osmolarity-dependent manner and reached peak levels of 12.55 ± 4.45 fold by 450 mOsM and 14.62 ± 3.79 fold by 500 mOsM, when compared to isosmolar controls (Fig. 2B). This pattern of TNF-α response to hyperosmolarity was confirmed at the protein level by ELISA. As shown in Fig. 2C, TNF-α protein concentration was low at 15.97 ± 2.58 pg/ml in cells cultured in isosmolar medium, but increased to 60.52 ± 10.97, 155.04 ± 17.21, and 167.87 ± 22.78 pg/ml, respectively, in cells treated with hyperosmolar medium at 400, 450 and 500 mOsM.

In contrast, the expression of the anti-inflammatory cytokine IL-37 was largely suppressed in HCECs exposed to hyperosmolarity. A time-course study showed that IL-37 mRNA levels decreased as early at 2 h reaching its lowest level of 43.75% at 4 h, then rebounding at 24 h in cells exposed to 450 mOsM medium (Fig. 2D). IL-37 mRNA levels were suppressed in an osmolarity-dependent manner with expression reduced to 45.0% by 450 mOsm and 43.0% by 500 mOsM (Fig. 2E). IL-37 protein concentration was 2.22 ± 0.44 ng/mg in HCECs in isosmolar controls, and it was significantly and osmolarity-dependently inhibited to 68.5, 47.7, and 46.8% by 400, 450 and 500 mOsM hyperosmolar media, respectively (Fig. 2F). These results suggest that stimulated TNF-α expression accompanied by suppressed IL-37 levels may be a novel mechanism by which hyperosmolarity induces inflammation and disrupts corneal epithelial barrier integrity.

3.3. Cysteine protease cathepsin S directly disrupted corneal epithelial barrier

Cathepsin S is a member of the peptidase C1 family encoded by CTSS gene [47]. Cathepsin S is known to degrade collagen and elastin [48], but its activity on tight junction proteins has not been studied, and it is largely unknown whether cathepsin S mediates epithelial barrier function. To explore the effects of CTSS on corneal epithelial barrier integrity, cathepsin S at different concentration (100–400 ng/ml) was added to isosmolar medium in HCEC cultures for 48 h. As shown in Fig. 3, the integrity of tight junction proteins, ZO-1 and occludin, was directly disrupted by cathepsin S in a concentration-dependent fashion from 100 to 400 ng/ml without hyperosmolar stress. To confirm its activity on barrier disruption, HCECs were incubated in 200 ng/ml of cathepsin S together with 50 μM of LY3000328, a cathepsin S inhibitor [49], for 48 h. We observed that LY3000328 largely restored the integrity of ZO-1 and occludin proteins, which were disrupted by cathepsin S.

3.4. Cathepsin S activity was stimulated by TNF-α

TNF-α has been reported to be involved in epithelial barrier disruption [50,51]. However, it is unknown whether TNF-α disrupts corneal epithelial barrier by stimulating cathepsin S production. The dose-dependent effects were determined of rhTNF-α on CTSS gene and protein expression levels. As shown in Fig. 4A, CTSS mRNA expression was stimulated significantly to 1.47 ± 0.48, 2.07 ± 0.43, and 2.09 ± 0.29 fold by TNF-α at 5, 10 and 20 ng/ml, respectively. Cathepsin S protein was observed to be constitutively produced and secreted by HCECs at a baseline level of 4.84 ± 0.67 ng/ml in medium as quantified by ELISA. Exogenous rhTNF-α at 5, 10 and 20 ng/ml stimulated the cathepsin S protein concentration in medium to 6.41 ± 0.35, 7.83 ± 0.59, and 9.01 ± 0.11 ng/ml, representing

1.32, 1.62 and 1.86 fold increase, respectively (Fig. 4B). Immunofluorescent staining further confirmed that cathepsin S immunoreactive intensity and number of positive cells increased significantly in HCECs treated by rhTNF-α at 10 and 20 ng/ml (Fig. 4C).

3.5. Anti-inflammatory cytokine IL-37 inhibited TNF-α production in HCECs exposed to hyperosmolar stress

We have shown that hyperosmolarity stimulates TNF-α at mRNA and protein levels in HCECs. To explore the anti-inflammatory role of IL-37, HCECs were treated with hyperosmolar medium, with or without exogenous rhIL-37 at different concentrations. Compared with isosmolar controls, TNF-α mRNA levels dramatically increased to 14.11 ± 3.49 fold by 450 mOsM, but significantly decreased to 7.52 ± 0.26, 5.10 ± 2.31, and 4.70 ± 1.99 fold, respectively, with addition of IL-37 at 5, 10 and 20 ng/ml, representing 46.7, 63.8, and 66.7% inhibition (Fig. 5A). ELISA results confirmed the inhibitory effect of IL-37 on TNF-α expression at the protein level. As shown in Fig. 5B, TNF-α protein level increased significantly to 146.6 ± 24.9 pg/ml by 450 mOsM, but it was largely inhibited to 80.04 ± 17.67, 63.41 ± 25.91, and 56.42 ± 18.53 pg/ml by addition of rhIL-37 at 5, 10 or 20 ng/ml, respectively, representing 45.4, 56.8 and 61.5% inhibition. Immunofluorescent staining further confirmed that the staining intensity and number of TNF-α positive cells increased significantly in HCECs at 450 mOsM, but also dramatically reduced by addition of rhIL-37 at 10 ng/ml (Fig. 5C).

3.6. IL-37 further suppressed hyperosmolarity stimulated cathepsin S production in HCECs

We have shown that cathepsin S production was stimulated by TNF-α, which was known to be induced by hyperosmolarity. To explore whether CTSS expression is also activated by hyperosmolarity, HCECs were treated with medium of increasing osmolarity. As shown in Fig. 6A, CTSS gene expression was osmolarity-dependently induced to 1.64 ± 0.18, 1.97 ± 0.49, and 1.94 ± 0.36 fold by medium at 400, 450 and 500 mOsM, respectively. Consistently, the basal cathepsin S concentration of 5.74 ± 0.75 ng/ml increased to 9.23 ± 4.09, 14.59 ± 2.79, and 16.36 ± 1.31 ng/ml, representing 1.62, 2.56, and 2.87 fold increases, respectively, in response to 400, 450, and 500 mOsM (Fig. 6B).

Interestingly, the hyperosmolarity-induced expression and production of cathepsin S in HCECs were largely suppressed by exogenous rhIL-37. As shown in Fig. 6C, the increased CTSS mRNA levels induced by 450 mOsM medium were largely abolished to 1.23 ± 0.55, 0.91 ± 0.3 and 0.80 ± 0.43 fold, respectively, with addition of IL-37 at 5, 10 and 20 ng/ml, representing 37.9, 54.6 and 59.6% inhibition.

ELISA results confirmed the inhibitory effect of IL-37 on cathepsin S expression at the protein level. As shown in Fig. 6D, the cathepsin S concentration of 5.70 ± 0.76 ng/ml in isosmolar medium increased to 13.7 ± 4.07 ng/ml by 450 mOsM, which was largely suppressed to 11.82 ± 1.78, 8.78 ± 2.84, and 8.17 ± 1.54 pg/ml by IL-37 at 5, 10 or 20 ng/ml, respectively, representing 13.7, 35.91, and 40.36% inhibition. Immunofluorescent staining further confirmed that the staining intensity and number of cathepsin S positive cells

significantly increased in HCECs at 450 mOsM, but were reduced by addition of rhIL-37 at 10 ng/ml (Fig. 6E).

3.7. IL-37 restored integrity of epithelial barrier in HCECs under hyperosmolar stress

We have shown that TNF-α significantly induces the expression of cathepsin S, which directly disrupts corneal epithelial barrier proteins, and that IL-37 suppresses the production of TNF-α and cathepsin S, which are stimulated by hyperosmolarity in HCECs. Does IL-37 protect against hyperosmolarity induced corneal epithelial barrier disruption?

To answer this question, HCECs were switched to 450 mOsM medium with or without IL-37 for 48 h before performing immunofluorescent staining. As shown in Fig. 7A with 2D and 3D images of laser confocal scanning microscopy, the integrity of ZO-1 protein was largely disrupted by hyperosmolar medium at 450 mOsM, but was almost restored morphologically following the addition of 10 ng/ml of rhIL-37. Occludin and claudin-1 immunostaining showed a similar response to hyperosmolarity. They were disrupted by 450 mOsM, but largely restored by co-incubation with IL-37 (Fig. 7 B and C). The immunoreactivity of the adheren junction protein E-cadherin was observed in cell membranes between cells in HCECs in isosmolar medium. The integrity of E-cadherin protein was largely disrupted in cells exposed to 450 mOsM, but was significantly restored by adding rhIL-37 in cells exposed to this hyperosmolar stress.

4. Discussion

Intact skin and mucosal barriers are crucial for maintaining tissue homeostasis, as they protect host tissues from a variety of environmental pathogens. Defective epithelial barriers are not only associated with allergic, autoimmune and inflammatory conditions in local tissues, but also affect remote tissues and systemic diseases (see review article [16, 52]). Ocular epithelial barrier disruption has been recognized as an important factor contributing to corneal epithelial disease, the common ocular surface inflammatory disease, dry eye [18,53].

Using an in vitro dry eye model of HCEC cultures exposed to hyperosmotic stress, we observed an interesting phenomenon that the anti-inflammatory IL-36 receptor antagonist IL-36RA and IL-38 suppress TNF-α and IL-1β production and protect tight junction barrier integrity from disruption by pro-inflammatory cytokine IL-36α and hyperosmolarity [54]. A recent study reported that the disruption of corneal epithelial tight junction proteins was associated with upregulation of TNF-α and matrix metalloproteinases in primary HCECs under hyperosmolarity stress [55]. In this study, we explored the novel role and molecular mechanism of a natural anti-inflammatory cytokine IL-37 in protecting corneal epithelial barrier using an in vitro dry eye model with hyperosmolar stress.

Mucosal epithelial cells form a barrier to the outside world with apical junctional complexes, which consist of the apical tight junctions and underlying adheren junctions that bind together through homotypic and heterotypic interactions, which not only maintain cell-to-cell contact but also construct cell polarity, and regulate the paracellular movement of ions and macromolecules [56–59]. Tight junction complexes are composed of transmembrane

proteins, such as claudins, occludin, and membrane-associated proteins ZO-1, -2, and -3. Adheren junctions are essential for tethering forces generated between the adjacent cells. Adheren junctions consist of a transmembrane protein E-cadherin and cytoplasmic linker proteins catenin α, β, γ. Three tight junction and one adheren junction proteins were evaluated in this study.

First, we observed that the integrity of major epithelial barrier proteins, ZO-1, occludin, claudin-1 and E-cadherin, was disrupted in HCECs exposed to hyperosmolar stress in a time- and osmolarity-dependently manner (Fig. 1). The findings suggest that corneal epithelial barrier disruption stimulated by hyperosmotic stress is an important pathogenic feature in dry eye.

Next, we revealed the opposite responses in expression of the pro- and anti-inflammatory cytokines, TNF-α and IL-37, to hyperosmolarity in HCECs. TNF-α was dramatically stimulated by hyperosmolar stress, which is consistent with our previous reports [60]. The expression and production of IL-37, a natural anti-inflammatory cytokine [22], was evident in HCECs by RT-qPCR and ELISA. The mRNA expression and protein production of IL-37 were significantly and osmolarity-dependently suppressed at the mRNA and protein levels in HCECs under hyperosmolar stress (Fig. 2).

These results reveal the imbalance in production of pro- and anti-inflammatory cytokines, with upregulated TNF-α and downregulated IL-37, in HCECs under hyperosmolar stress. The findings suggest that suppression of IL-37 by hyperosmolarity may contribute to the pathogenesis of inflammatory dry eye disease mediated corneal barrier disruption. Detection of IL-37 production by human corneal epithelium encouraged us to investigate whether IL-37 could protect corneal cells from barrier disruption induced by hyperosmolarity, which is a core mechanism of dry eye diseases [50].

By searching for enzymes that could directly disrupt epithelial barrier, a cysteine protease cathepsin S was observed to be a good candidate that may be involved in corneal barrier disruption in dry eye conditions. Cathepsin S, encoded by CTSS gene, is mainly found inside the lysosomal/endosomal compartments of antigen-presenting cells, and is also produced by epithelial cells. It plays an important role in intracellular and extracellular processes, such as proteolysis [47,61]. Cathepsin S is known to be able to degrade collagen and elastin [48], but its ability to disrupt tight junction and adheren junction proteins has not been studied. Furthermore, increased cathepsin S activity has been detected in tear fluid from patients with Sjogren's syndrome [61].

We observed that exogenous cathepsin S directly disrupted the integrity of tight junction proteins ZO-1 and occludin in HCECs. This disruptive effect of cathepsin S was confirmed by LY3000328, a cathepsin S inhibitor [49], which completely restored the integrity of tight junction proteins (Fig. 3). CTSS expression and cathepsin S production in HCECs were significantly stimulated by TNF-α (Fig. 4) and hyperosmolarity (Fig. 6 A and B), the latter also stimulating TNF-α mRNA and protein (Fig. 2A–C). The findings suggest TNF-α/CTSS signaling contributes to barrier disruption in HCECs exposed to hyperosmolar stress.

To explore the protective function and mechanism of IL-37, we performed three additional studies. First, we observed that rhIL-37 at 5–20 ng/ml significantly inhibited TNF-α production at mRNA and protein levels induced by hyperosmolarity (Fig. 5). Further, we showed that exogenous rhIL-37 significantly blocked the expression and production of cathepsin S stimulated by hyperosmolarity in HCECs (Fig. 6C and D). This suggests that IL-37 blocked CTSS expression via inhibiting TNF-α production induced by hyperosmolarity. Furthermore, we confirmed that rhIL-37 largely restored the integrity of major barrier proteins, including tight junctions ZO-1, occludin and claudin-1, and adheren junction E-cadherin, which were disrupted under hyperosmolar stress in HCECs, as shown in 2D and 3D confocal microscopy images (Fig. 7).

This study for the first time introduces a natural anti-inflammatory cytokine IL-37 in the field of dry eye associated ocular surface inflammatory disease. The findings are limited to the role of IL-37 in protecting corneal epithelial barrier from hyperosmolar stress using an in vitro dry eye model. Further investigations are needed to provide greater insight into IL-37 in dry eye pathogenesis and its therapeutic potential.

In conclusion, our findings demonstrate that the suppressed anti-inflammatory cytokine IL-37 combined with the stimulated proinflammatory cytokine TNF-α and protease cathepsin S provides a novel mechanism by which hyperosmolar stress disrupts corneal barrier proteins, an important inflammatory mediated mechanism in dry eye induced corneal epithelial disease. Exogenous IL-37 is capable of restoring the integrity of corneal barrier proteins via inhibition of TNF-α/CTSS signaling in HCECs under hyperosmolar stress.

Acknowledgements

This work is supported by grants from NIH, NEI, EY023598 (DQL), EY011915 (SCP), EY030447 (CSDP), and EY002520 (Core Grant for Vision Research), AbbVie Inc., Lions Foundation for Sight (YZ and JML), Research to Prevent Blindness, The Hamill Foundation.

We thank Drs. Marshall Bowes Hamill and Alice Matoba for their kind support and the Lions Eye Bank of Texas for providing human corneoscleral tissues.

References

[1]. Steelant B, Seys SF, Van Gerven L, Van Woensel M, Farre R, Wawrzyniak P, et al. Histamine and t helper cytokine-driven epithelial barrier dysfunction in allergic rhinitis. J Allergy Clin Immunol 2018;141:951–63. e8. [PubMed: 29074456]

[2]. Georas SN, Rezaee F. Epithelial barrier function: at the front line of asthma immunology and allergic airway inflammation. J Allergy Clin Immunol 2014;134:509–20. [PubMed: 25085341]

[3]. Heijink IH, Nawijn MC, Hackett TL. Airway epithelial barrier function regulates the pathogenesis of allergic asthma. Clin Exp Allergy 2014;44:620–30. [PubMed: 24612268]

[4]. Chen JC, Chuang JG, Su YY, Chiang BL, Lin YS, Chow LP. The protease allergen pen c 13 induces allergic airway inflammation and changes in epithelial barrier integrity and function in a murine model. J Biol Chem 2011;286:26667–79. [PubMed: 21613216]

[5]. O'Regan GM, Irvine AD. The role of filaggrin in the atopic diathesis. Clin Exp Allergy 2010;40:965–72. [PubMed: 20642575]

[6]. Demehri S, Morimoto M, Holtzman MJ, Kopan R. Skin-derived tslp triggers progression from epidermal-barrier defects to asthma. PLoS Biol 2009;7:e1000067. [PubMed: 19557146]

[7]. Rochman M, Travers J, Abonia JP, Caldwell JM, Rothenberg ME. Synaptopodin is upregulated by il-13 in eosinophilic esophagitis and regulates esophageal epithelial cell motility and barrier integrity. JCI Insight 2017;2:e96789. [PubMed: 29046486]

[8]. Zimmerman NP, Vongsa RA, Wendt MK, Dwinell MB. Chemokines and chemokine receptors in mucosal homeostasis at the intestinal epithelial barrier in inflammatory bowel disease. Inflamm Bowel Dis 2008;14:1000–11. [PubMed: 18452220]

[9]. Martin A, Devkota S. Hold the door: role of the gut barrier in diabetes. Cell Metabol 2018;27:949–51.

[10]. Bahlouli W, Breton J, Lelouard M, L'Huillier C, Tirelle P, Salameh E, et al. Stress-induced intestinal barrier dysfunction is exacerbated during diet-induced obesity. J Nutr Biochem 2020;81:108382. [PubMed: 32417626]

[11]. Flak MB, Colas RA, Munoz-Atienza E, Curtis MA, Dalli J, Pitzalis C. Inflammatory arthritis disrupts gut resolution mechanisms, promoting barrier breakdown by porphyromonas gingivalis. JCI Insight 2019;4:e125191. [PubMed: 31292292]

[12]. Kim JW, Kwok SK, Choe JY, Park SH. Recent advances in our understanding of the link between the intestinal microbiota and systemic lupus erythematosus. Int J Mol Sci 2019;20:4871. [PubMed: 31575045]

[13]. Kelly JR, Kennedy PJ, Cryan JF, Dinan TG, Clarke G, Hyland NP. Breaking down the barriers: the gut microbiome, intestinal permeability and stress-related psychiatric disorders. Front Cell Neurosci 2015;9:392. [PubMed: 26528128]

[14]. van ISCD, Derkinderen P. The intestinal barrier in Parkinson's disease: current state of knowledge. J Parkinsons Dis 2019;9:S323–9. [PubMed: 31561386]

[15]. Kohler CA, Maes M, Slyepchenko A, Berk M, Solmi M, Lanctot KL, et al. The gut-brain axis, including the microbiome, leaky gut and bacterial translocation: mechanisms and pathophysiological role in alzheimer's disease. Curr Pharmaceut Des 2016;22:6152–66.

[16]. Akdis CA. Does the epithelial barrier hypothesis explain the increase in allergy, autoimmunity and other chronic conditions? Nat Rev Immunol 2021;21:739–51. [PubMed: 33846604]

[17]. Yamaguchi T Inflammatory response in dry eye. Invest Ophthalmol Vis Sci 2018;59:DES192–9. [PubMed: 30481826]

[18]. Pflugfelder SC, de Paiva CS. The pathophysiology of dry eye disease: what we know and future directions for research. Ophthalmology 2017;124:S4–13. [PubMed: 29055361]

[19]. Paiva CS, Pflugfelder SC. Rationale for anti-inflammatory therapy in dry eye syndrome. Arq Bras Oftalmol 2008;71:89–95. [PubMed: 19274418]

[20]. Calonge M, Enriquez-de-Salamanca A. The role of the conjunctival epithelium in ocular allergy. Curr Opin Allergy Clin Immunol 2005;5:441–5. [PubMed: 16131921]

[21]. Hu J, Gao N, Zhang Y, Chen X, Li J, Bian F, et al. Il-33/st2/il-9/il-9r signaling disrupts ocular surface barrier in allergic inflammation. Mucosal Immunol 2020;13:919–30. [PubMed: 32358573]

[22]. Tete S, Tripodi D, Rosati M, Conti F, Maccauro G, Saggini A, et al. Il-37 (il-1f7) the newest anti-inflammatory cytokine which suppresses immune responses and inflammation. Int J Immunopathol Pharmacol 2012;25:31–8. [PubMed: 22507315]

[23]. Boraschi D, Lucchesi D, Hainzl S, Leitner M, Maier E, Mangelberger D, et al. Il-37: a new anti-inflammatory cytokine of the il-1 family. Eur Cytokine Netw 2011;22:127–47. [PubMed: 22047735]

[24]. Wegmann M Targeting cytokines in asthma therapy: could il-37 be a solution? Expet Rev Respir Med 2017;11:675–7.

[25]. Lunding L, Webering S, Vock C, Schroder A, Raedler D, Schaub B, et al. Effect of il-37 on allergic airway inflammation. Ann Am Thorac Soc 2016;13(Suppl 1):S95–6.

[26]. Xu WD, Zhao Y, Liu Y. Insights into il-37, the role in autoimmune diseases. Autoimmun Rev 2015;14:1170–5. [PubMed: 26264940]

[27]. Weidlich S, Bulau AM, Schwerd T, Althans J, Kappler R, Koletzko S, et al. Intestinal expression of the anti-inflammatory interleukin-1 homologue il-37 in pediatric inflammatory bowel disease. J Pediatr Gastroenterol Nutr 2014;59:e18–26. [PubMed: 24732025]

[28]. Teng X, Hu Z, Wei X, Wang Z, Guan T, Liu N, et al. Il-37 ameliorates the inflammatory process in psoriasis by suppressing proinflammatory cytokine production. J Immunol 2014;192:1815–23. [PubMed: 24453242]

[29]. McNamee EN, Masterson JC, Jedlicka P, McManus M, Grenz A, Collins CB, et al. Interleukin 37 expression protects mice from colitis. Proc Natl Acad Sci USA 2011;108:16711–6. [PubMed: 21873195]

[30]. Abulkhir A, Samarani S, Amre D, Duval M, Haddad E, Sinnett D, et al. A protective role of il-37 in cancer: a new hope for cancer patients. J Leukoc Biol 2017;101:395–406. [PubMed: 27881603]

[31]. Ding VA, Zhu Z, Xiao H, Wakefield MR, Bai Q, Fang Y. The role of il-37 in cancer. Med Oncol 2016;33:68. [PubMed: 27251377]

[32]. Kim HS, Jun SX, de Paiva CS, Chen Z, Pflugfelder SC, Li D-Q. Phenotypic characterization of human corneal epithelial cells expanded ex vivo from limbal explant and single cell cultures. Exp Eye Res 2004;79:41–9. [PubMed: 15183099]

[33]. Li DQ, Chen Z, Song XJ, Luo L, Pflugfelder SC. Stimulation of matrix metalloproteinases by hyperosmolarity via a jnk pathway in human corneal epithelial cells. Invest Ophthalmol Vis Sci 2004;45:4302–11. [PubMed: 15557436]

[34]. Liu Z, Chen D, Chen X, Bian F, Qin W, Gao N, et al. Trehalose induces autophagy against inflammation by activating tfeb signaling pathway in human corneal epithelial cells exposed to hyperosmotic stress. Invest Ophthalmol Vis Sci 2020;61:26.

[35]. Li DQ, Kim S, Li JM, Gao Q, Choi J, Bian F, et al. Single-cell transcriptomics identifies limbal stem cell population and cell types mapping its differentiation trajectory in limbal basal epithelium of human cornea. Ocul Surf 2021;20:20–32. [PubMed: 33388438]

[36]. Li D-Q, Chen Z, Song XJ, Luo L, Pflugfelder SC. Stimulation of matrix metalloproteinases by hyperosmolarity via a jnk pathway in human corneal epithelial cells. Invest Ophthalmol Vis Sci 2004;45:4302–11. [PubMed: 15557436]

[37]. Li D-Q, Luo L, Chen Z, Kim HS, Song XJ, Pflugfelder SC. Jnk and erk map kinases mediate induction of il-1beta, tnf-alpha and il-8 following hyperosmolar stress in human limbal epithelial cells. Exp Eye Res 2006;82:588–96. [PubMed: 16202406]

[38]. Liu Z, Chen D, Chen X, Bian F, Gao N, Li J, et al. Autophagy activation protects ocular surface from inflammation in a dry eye model in vitro. Int J Mol Sci 2020;21:8966. [PubMed: 33255884]

[39]. Chi W, Hua X, Chen X, Bian F, Yuan X, Zhang L, et al. Mitochondrial DNA oxidation induces imbalanced activity of nlrp3/nlrp6 inflammasomes by activation of caspase-8 and brcc36 in dry eye. J Autoimmun 2017;80:65–76. [PubMed: 28238526]

[40]. Hua X, Deng R, Li J, Chi W, Su Z, Lin J, et al. Protective effects of l-carnitine against oxidative injury by hyperosmolarity in human corneal epithelial cells. Invest Ophthalmol Vis Sci 2015;56:5503–11. [PubMed: 26284556]

[41]. Ong YL, Irvine A. Quantitative real-time pcr: a critique of method and practical considerations. Hematology 2002;7:59–67. [PubMed: 12171779]

[42]. Li DQ, Zhou N, Zhang L, Ma P, Pflugfelder SC. Suppressive effects of azithromycin on zymosan-induced production of proinflammatory mediators by human corneal epithelial cells. Invest Ophthalmol Vis Sci 2010;51:5623–9. [PubMed: 20538995]

[43]. Markov AG, Aschenbach JR, Amasheh S. Claudin clusters as determinants of epithelial barrier function. IUBMB Life 2015;67:29–35. [PubMed: 25788154]

[44]. Ivanov AI, Parkos CA, Nusrat A. Cytoskeletal regulation of epithelial barrier function during inflammation. Am J Pathol 2010;177:512–24. [PubMed: 20581053]

[45]. Yu QH, Yang Q. Diversity of tight junctions (tjs) between gastrointestinal epithelial cells and their function in maintaining the mucosal barrier. Cell Biol Int 2009;33:78–82. [PubMed: 18938254]

[46]. Wang JY. Polyamines regulate expression of e-cadherin and play an important role in control of intestinal epithelial barrier function. Inflammopharmacology 2005;13:91–101. [PubMed: 16259731]

[47]. Gupta S, Singh RK, Dastidar S, Ray A. Cysteine cathepsin s as an immunomodulatory target: present and future trends. Expert Opin Ther Targets 2008;12:291–9. [PubMed: 18269339]

[48]. Vidak E, Javoršek U, Vizovišek M, Turk B. Cysteine cathepsins and their extracellular roles: shaping the microenvironment. Cells 2019;8. [PubMed: 31861404]

[49]. Payne CD, Deeg MA, Chan M, Tan LH, LaBell ES, Shen T, et al. Pharmacokinetics and pharmacodynamics of the cathepsin s inhibitor, ly3000328, in healthy subjects. Br J Clin Pharmacol 2014;78:1334–42. [PubMed: 25039273]

[50]. Rajashekhar G, Shivanna M, Kompella UB, Wang Y, Srinivas SP. Role of mmp-9 in the breakdown of barrier integrity of the corneal endothelium in response to tnf-alpha. Exp Eye Res 2014;122:77–85. [PubMed: 24667088]

[51]. Kimura K, Morita Y, Orita T, Haruta J, Takeji Y, Sonoda KH. Protection of human corneal epithelial cells from tnf-alpha-induced disruption of barrier function by rebamipide. Invest Ophthalmol Vis Sci 2013;54:2572–760. [PubMed: 23482463]

[52]. Pat Y, Ogulur I. The epithelial barrier hypothesis: a 20-year journey. Allergy 2021;76:3560–2. [PubMed: 33982305]

[53]. Bron AJ, de Paiva CS, Chauhan SK, Bonini S, Gabison EE, Jain S, et al. Tfos dews ii pathophysiology report. Ocul Surf 2017;15:438–510. [PubMed: 28736340]

[54]. Li JM, Lu R, Zhang Y, Lin J, Hua X, Pflugfelder SC, et al. Il-36alpha/il-36ra/il-38 signaling mediates inflammation and barrier disruption in human corneal epithelial cells under hyperosmotic stress. Ocul Surf 2021;22:163–71. [PubMed: 34428579]

[55]. Zhang Y, Yang M, Zhao SX, Nie L, Shen LJ, Han W. Hyperosmolarity disrupts tight junction via tnf-alpha/mmp pathway in primary human corneal epithelial cells. Int J Ophthalmol 2022;15:683–9. [PubMed: 35601157]

[56]. Rezaee F, Georas SN. Breaking barriers. New insights into airway epithelial barrier function in health and disease. Am J Respir Cell Mol Biol 2014;50:857–69. [PubMed: 24467704]

[57]. Bardag-Gorce F, Hoft RH, Wood A, Oliva J, Niihara H, Makalinao A, et al. The role of e-cadherin in maintaining the barrier function of corneal epithelium after treatment with cultured autologous oral mucosa epithelial cell sheet grafts for limbal stem deficiency. J Ophthalmol 2016;2016:4805986. [PubMed: 27777792]

[58]. Ortiz-Melo MT, Sanchez-Guzman E, Gonzalez-Robles A, Valdes J, Gomez-Flores E, Castro-Munozledo F. Expression of claudins -2 and -4 and cingulin is coordinated with the start of stratification and differentiation in corneal epithelial cells: retinoic acid reversibly disrupts epithelial barrier. Biol Open 2013;2:132–43. [PubMed: 23429425]

[59]. Ko JA, Yanai R, Nishida T. Up-regulation of zo-1 expression and barrier function in cultured human corneal epithelial cells by substance p. FEBS Lett 2009;583:2148–53. [PubMed: 19446555]

[60]. Li D-Q, Luo L, Chen Z, Kim HS, Song XJ, Pflugfelder SC. Jnk and erk map kinases mediate induction of il-1beta, tnf-alpha and il-8 following hyperosmolar stress in human limbal epithelial cells. Exp Eye Res 2006;82:588–96. [PubMed: 16202406]

[61]. Hamm-Alvarez SF, Janga SR, Edman MC, Madrigal S, Shah M, Frousiakis SE, et al. Tear cathepsin s as a candidate biomarker for sjogren's syndrome. Arthritis Rheumatol 2014;66:1872–81. [PubMed: 24644101]

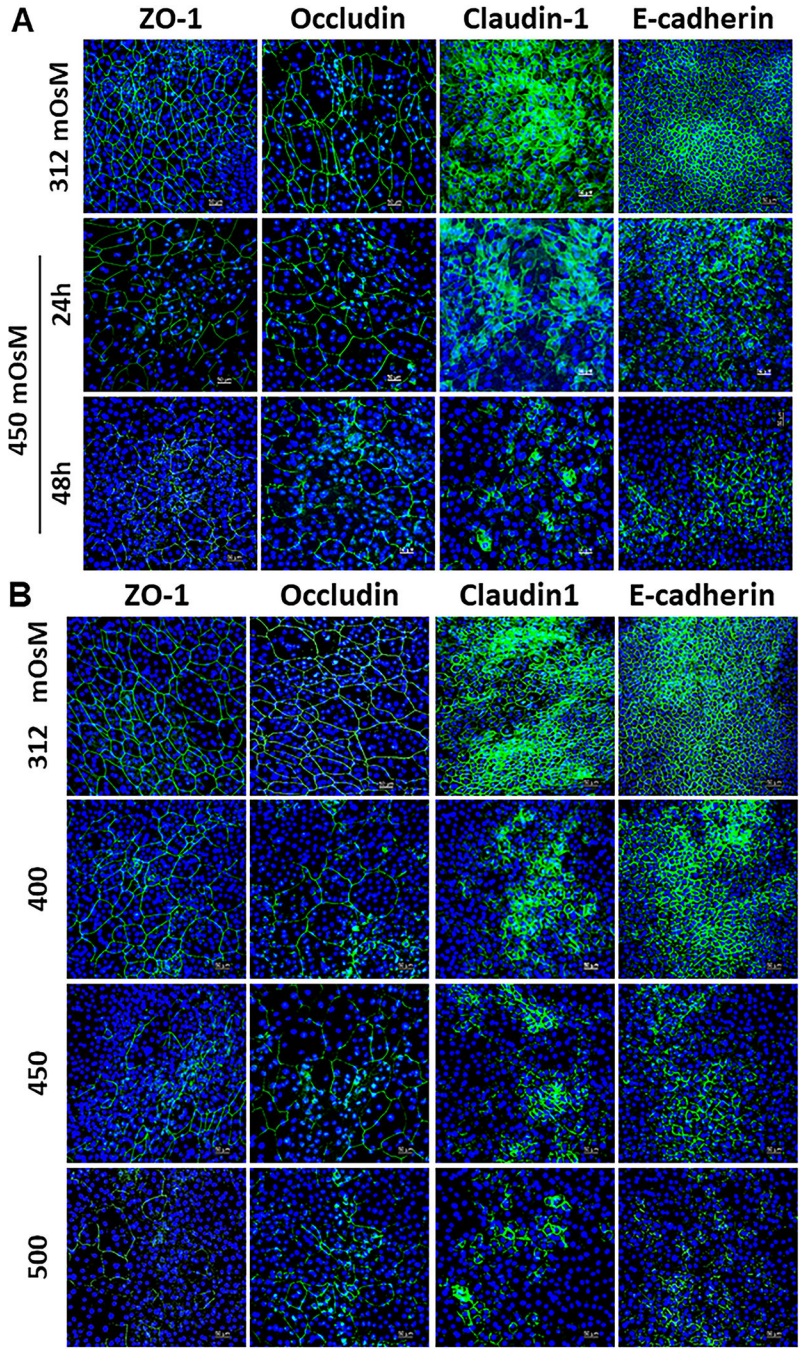

Fig. 1.

Corneal epithelial barrier was disrupted by hyperosmolar stress. Representative images of immunofluorescent staining showed that epithelial tight junction proteins ZO-1, occludin and claudin-1, as well as adheren junction E-cadherin were disrupted in HCECs exposed to hyperosmolar medium at 450mOsM for 24 and 48 h (**A**), and to hyperosmolar medium at 400, 450 and 500 mOsM for 48 h, with isosmolar medium (312 mOsM) as controls (**B**).

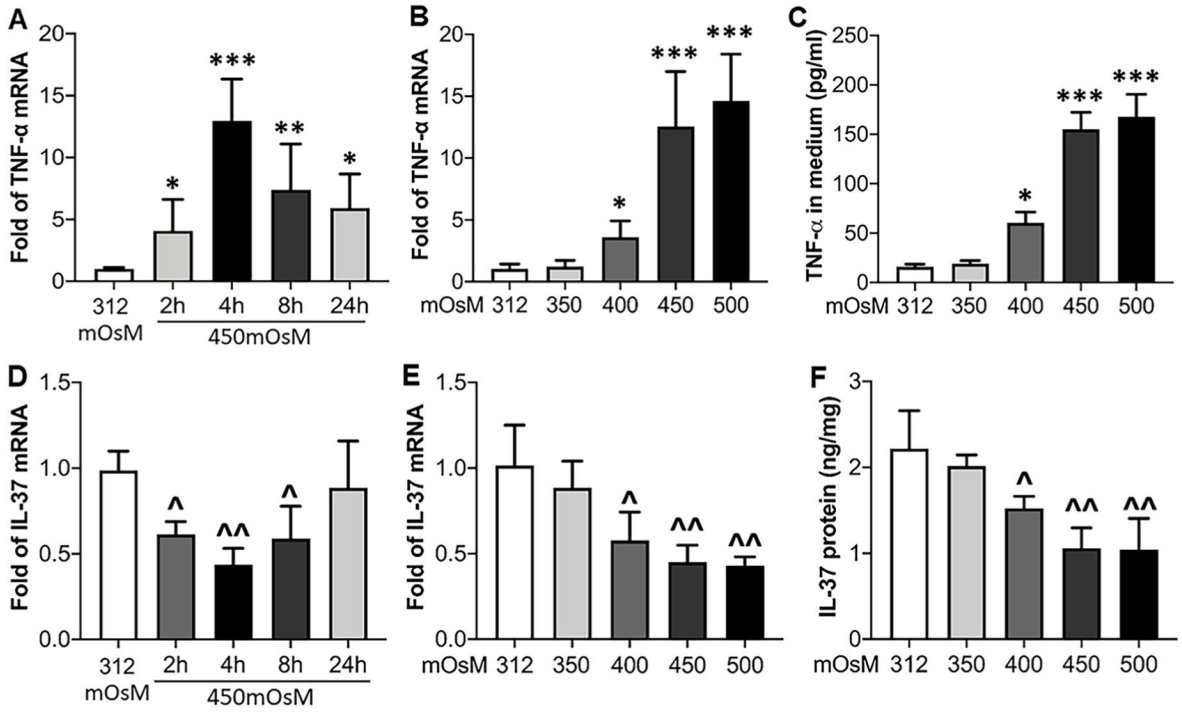

Fig. 2.

Opposite responses of TNF-α and IL-37 to hyperosmolarity. A. The time course of TNF-α mRNA expression, evaluated by RT-qPCR, in HCECs exposed to 450mOsM medium for 2, 4, 8, and 24 h, with isosmolar medium as control. **B.-C.** The dose-responses of TNF-α at the mRNA (**B**) and protein levels, evaluated by ELISA (**C**), in HCECs exposed to medium with increasing osmolarity (312, 350, 400, 450, and 500 mOsM). **D.** The time course of IL-37 mRNA expression in HCECs exposed to 450mOsM medium for 2, 4, 8, and 24 h, with isosmolar medium as control. **E.-F.** The dose-responses of IL-37 at the mRNA (**E**) and protein levels (**F**) in HCECs exposed to medium with increasing osmolarity (312, 350, 400, 450, and 500 mOsM). Data were summarized as mean ± SD from 5 separated experiments. **P < 0.05, **P < 0.01, ***P < 0.001,* as compared with controls at 312 mOsM; ^ *P < 0.05,* ^^ *P < 0.01,* as compared with 312 mOsM.

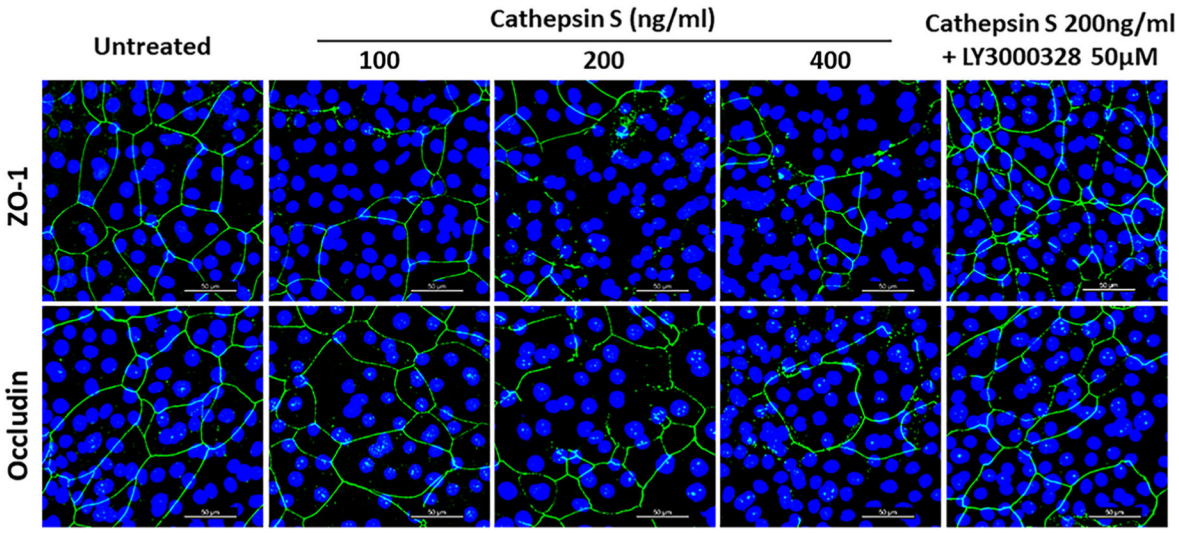

Fig. 3.

Cathepsin S directly disrupted corneal epithelial barrier. Representative images of immunofluorescent staining showed that tight junction proteins ZO-1 and occludin were dose-dependently disrupted in HCECs treated with increasing concentrations of cathepsin S at 100, 200 and 400 ng/ml for 48 h, when compared with untreated controls; and 50 μM of LY3000328, a cathepsin S inhibitor, protected these barrier proteins from disruption by 200 ng/ml of cathepsin S.

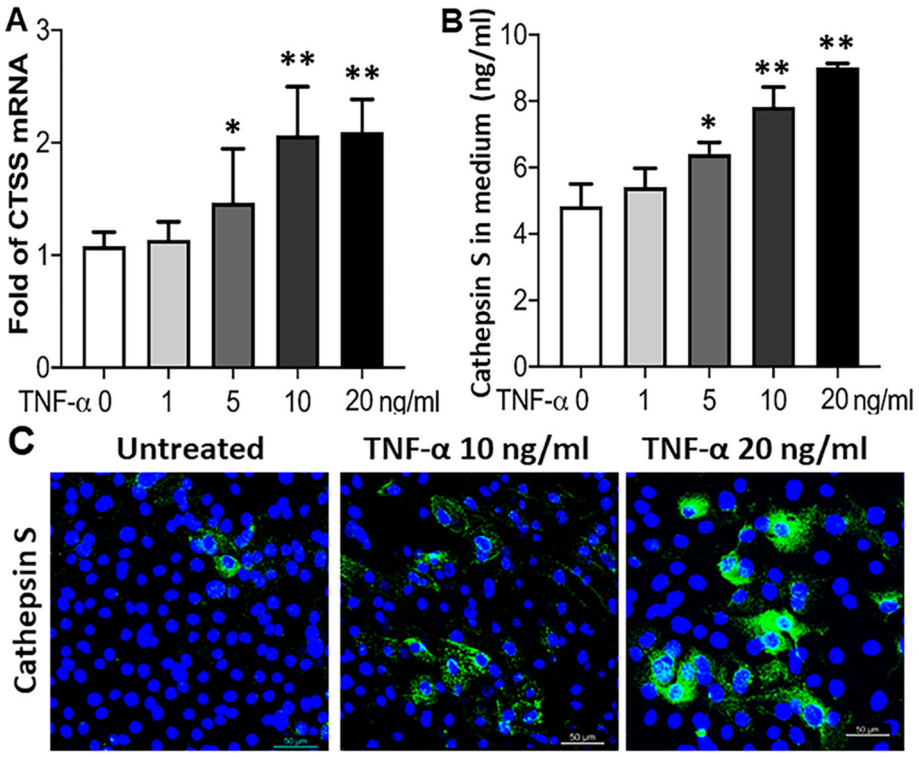

Fig. 4.

TNF-α stimulated the production of cathepsin S in HCECs. The expression of CTSS increased dose-dependently in HCECs treated with TNF-α at 1, 5, 10, 20 ng/ml, as evaluated at the mRNA by RT-qPCR (**A**) and protein levels by ELISA (**B**). Data were summarized as mean ± SD from 5 separated experiments. **P < 0.05, **P < 0.01,* as compared with untreated controls. **C.** Representative images of immunofluorescent staining confirmed that the immunoreactive intensity and number of cathepsin S positive cells increased in HCECs stimulated by TNF-α at 10–20 ng/ml.

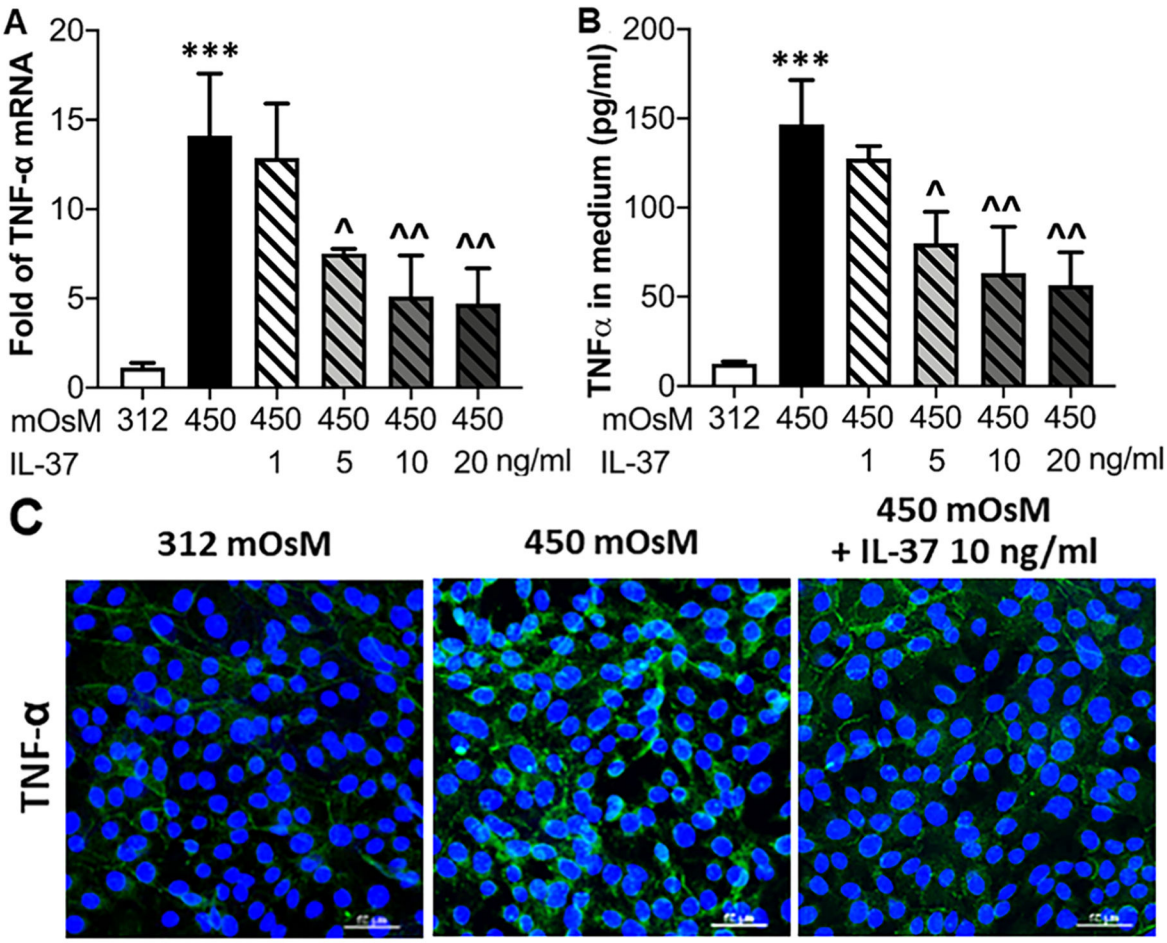

Fig. 5.

IL-37 inhibited the TNF-α expression in HCECs exposed to hyperosmolar stress. A.-B, The stimulated expression of TNF-α by hyperosmolar medium (450mOsM) was inhibited by rhIL-37 at 5, 10, and 20 ng/ml in HCECs, as evaluated at the mRNA by RT-qPCR (**A**) and protein levels by ELISA (**B**). Data were summarized as mean ± SD from 5 separated experiments. ****P < 0.001,* as compared with 312 mOsM controls; ^ *P < 0.05,* ^^ *P < 0.01,* as compared with hyperosmolar medium at 450 mOsM. **C.** Immunofluorescent staining showed that immunoreactive intensity and number of TNF-α positive cells increased in HCECs exposed to 450mOsM, but inhibited by addition of rhIL-37 (10 ng/ml).

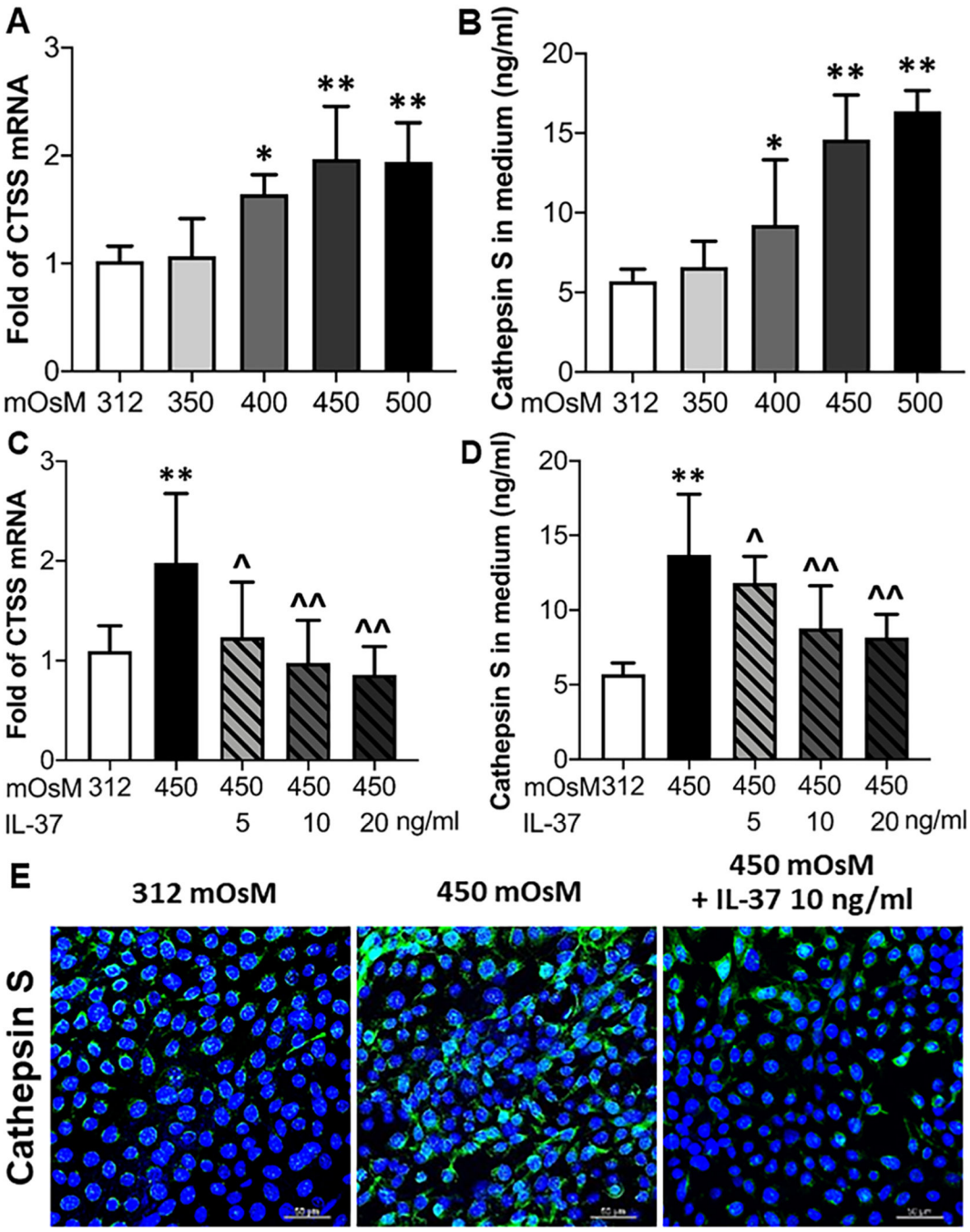

Fig. 6. IL-37 suppressed the CTSS expression under hyperosmolar stress.

A,-B. CTSS expression was osmolarity-dependently induced in HCECs exposed to medium at 400–500mOsM at the mRNA by RT-qPCR (**A**) and protein levels by ELISA (**B**). **C.-D.** The stimulated expression of CTSS by hyperosmolar medium (450mOsM) was suppressed by rhIL-37 at 5, 10, and 20 ng/ml in HCECs at the mRNA (**C**) and protein levels (**D**). Data were summarized as mean ± SD from 5 separated experiments. **P < 0.05, **P < 0.01,* as compared with 312 mOsM controls; ^ *P < 0.05,* ^^ *P < 0.01,* as compared with 450 mOsM. **E.** Immunofluorescent staining confirmed that immunoreactive intensity and

number of cathepsin S positive cells increased by hyperosmolar medium (450mOsM) and were suppressed by addition of rhIL-37 (10 ng/ml).

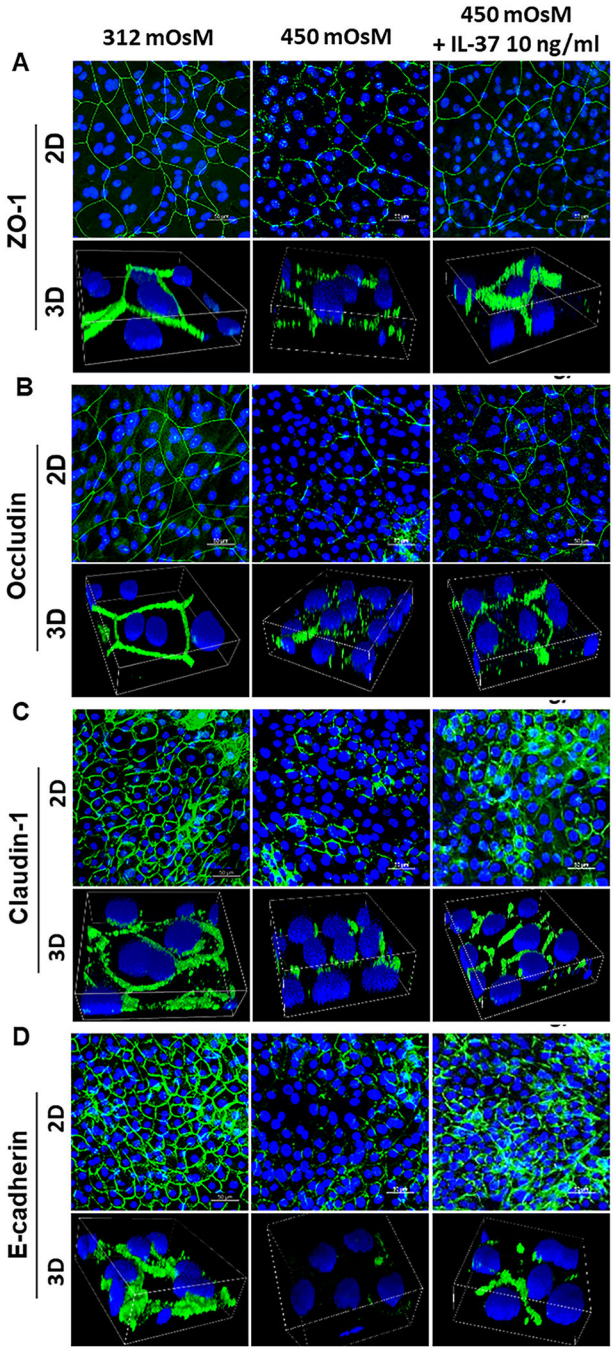

Fig. 7. IL-37 restored integrity of corneal epithelial barrier proteins disrupted by hyperosmolarity.

Representative 2D and 3D images of immunofluorescent staining showed that tight junction proteins, ZO-1 (**A**), occludin (**B**) and claudin-1 (**C**), and adheren junction E-cadherin **(D**) were significantly disrupted in HCECs exposed to hyperosmolar medium at 450 mOsM, but largely restored by addition of 10 ng/ml of rhIL-37.